RSC Nanoscale

ARTICLE

Synaptic plasticity, metaplasticity and memory effects in hybrid organic-inorganic bismuth-based materials

Tomasz Mazur, [†a]* Piotr Zawal[†b]* and Konrad Szaciłowski [a]

Supporting Information

1. Preparation of bismuth perovskite starting solutions

Weighted amounts of methylammonium iodide (M_{MAI} = 159 g/mol) were mixed with bismuth iodide (M_{BiI3} = 590 g/mol) and dissolved in 0.5 mL of N,N-dimethylformamide (DMF) with following molar ratios:

Table S1 Substrates used in MABiI thin films preparation.

MAI:BiI_3 ratio	mass of MAI	mass of BiI_3
1:3	26.5 mg	295.0 mg
1:1	79.5 mg	295.0 mg
3:2	59.6 mg	147.5 mg
3:1	159.0 mg	196.7 mg

2. UV-Vis spectra of pure precursors solutions in DMF

UV-Vis spectrum (325 nm – 800 nm) of pure MAI in DMF is characterized by one absorption maximum at 366 nm (MAI) and BiI_3 in DMF has a maximum at 435 nm, originating from $[BiI_4]^-$ complexes.

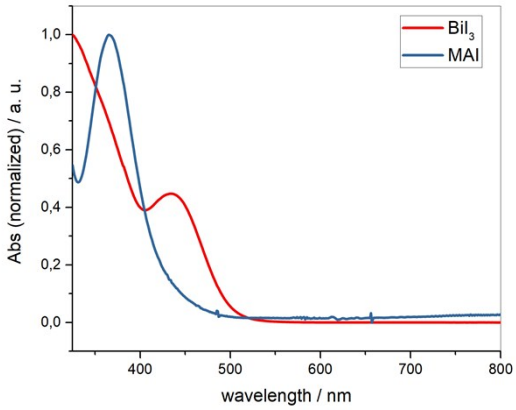

Figure S1 UV-Vis spectrum of pure precursors - methylammonium iodide (MAI) and bismuth triodide BiI_3 - dissolved in DMF.

3. Calculation of Schottky barrier height

To study the character of the interface we have employed the thermionic emission theory to extract the information from the I-V measurement curve. The Schottky character of the MABiI3/Cu junction is clearly visible while scanning from 0 V to 0.8 V. The reverse saturation current and the ideality factor can be calculated from the equation defining Schottky diode current for forward bias voltages:

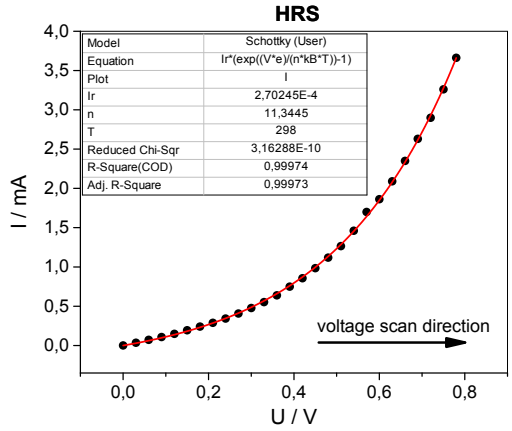

$$I_s = I_r\left(\exp\left(\frac{ev}{k_B T}\right) - 1\right) \quad (1)$$

Figure S2 Schottky diode-like I-V characteristics during forward voltage scan direction.

The fitting results are presented in Figure S2. The calculated saturation current is I_r = 0.27 mA and the ideality parameter is 11.35, indicating strong deviance from the ideal current values. This might originate from the fact, that investigated device is not just a pure diode, but rather can be described as a circuit. The character of the junction changes from Schottky-like to Ohmic when the memristor is in LRS (Figure S3).

One can exclude the filament formation, as the switching is not abrupt but rather changes gradually, which might result from changes in junction properties. Moreover, the prepared devices did not need any electroforming procedure in order to exhibit memristive behaviour, which is often necessary for memristors with filament resistive switching mechanism.[1] As mentioned before, the current flowing through the junction at the MABiI/Cu interface is not ideal (as indicated by the n parameter). To further investigate this behaviour we have focused only on one part of the loop, strongly resembling the Schottky diode characteristic (consisting of 0 V → +3 V and -3 V → 0 V parts of the I-V curve). Since the current

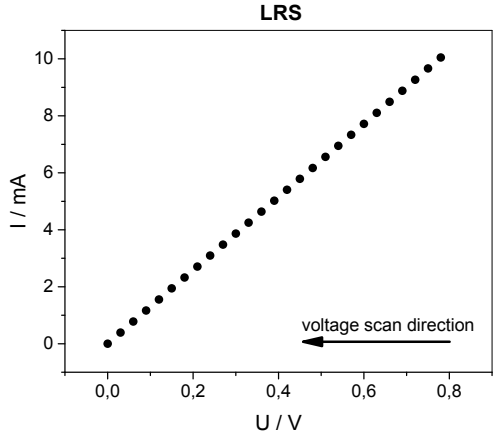

Figure S3 Ohmic I-V characteristic during the reverse voltage scan direction.

response differs from this for the ideal diode and the Ohmic component is present, we suggest that the junction acts not as a single diode, but rather a circuit as shown on the diagram in Figure S4:

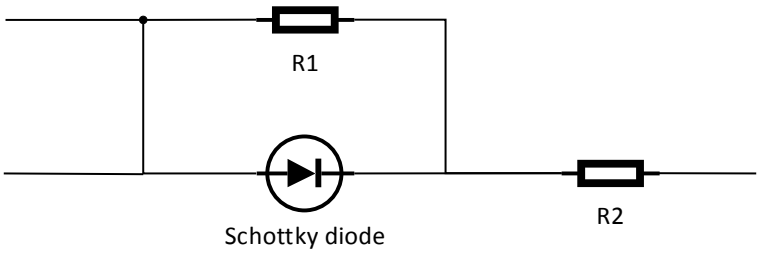

Figure S4 Equivalent circuit consisting of parallel connected Schottky diode and resistor R1 with additional resistor R2 in series. The former was used to take into the consideration the higher resistance of HRS.

When the diode is polarized with a forward bias, the total circuit resistance is approximately equal to R2. Under reverse bias polarization, the sum of two resistors determines the circuit resistance, which accounts for the transition to HRS. In order to calculate the resistance, the linear function has been fitted to both regions of the data (Figure S5).

In the HRS the function has been fitted only to the linear current response. The calculated resistances from slopes of fitted functions are: *R2* = 49.90 Ω (LRS part) and *R1+R2* = 689.66 Ω (HRS part), meaning *R1* = 639.76 Ω. To calculate the reverse saturation current, we have eliminated the Ohmic component by subtracting the theoretical current flowing through *R2* from the measured current values. As the *R2* resistance is present only in HRS, the correction was made only for voltages below the switching voltage, i.e. 0.8 V (as indicated in Figure S5 by the vertical line):

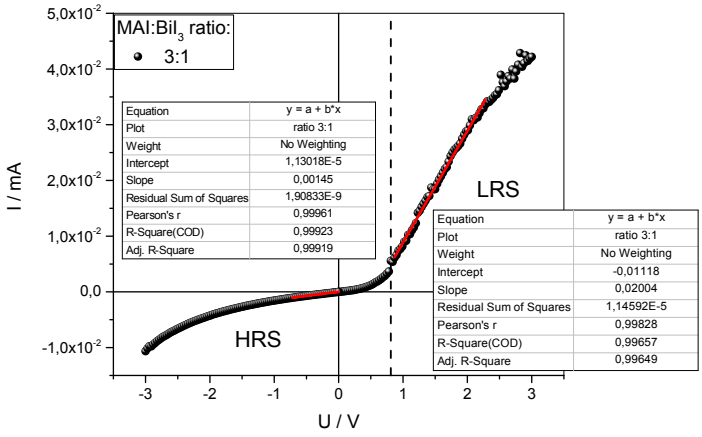

Figure S5 The fitting data of linear functions used to estimate resistance of R1 and R2. The functions were fitted to linear current response in both HRS and LRS to determine R1+R2 and R2, respectively.

These calculations led us to estimate the reverse saturation current of the diode to J_0 = 4.87×10-2 mA (calculated as the average current for voltages in the linear range from -1 V to 0 V). After these calculations, the Schottky barrier height can be calculated from the Richardson equation:

$$J_0 = A^* \cdot T^2 \exp\left(\frac{q_e \varphi_B}{kT}\right) \qquad (2)$$

where J_0 is the reverse saturation current, T is temperature, q_e is the elementary charge, φ_B is Schottky barrier height, k is the Boltzmann constant and A^* is the effective Richardson constant defined as follows: $A^* = 4\pi q_e m_e^* k^2 h^{-3}$, where m_e^* is the electron effective mass and h is the Planck constant. In $MA_3Bi_2I_9$ the effective mass $m_e^*_{A\text{-}H}$ was calculated to be 0.54[2] and the temperature at which the measurements were conducted was 23 °C. Thus, the calculated Schottky barrier height on the MABI/Cu junction is φ_B = 0.55 eV. We have additionaly investigated the Schottky barrier with Ultraviolet Photoelectron Spectroscopy (UPS). The measured barrier height was 0.5 V on MABiI/Cu interface, whereas at MABiI/PEDOT:PSS interface the height was 0 V, indicating Ohmic type of this junction.

4. Simple neuromorphic functions – learning and forgetting (fitting data)

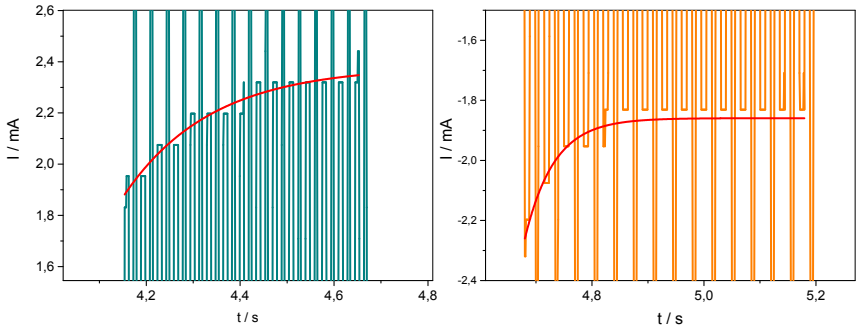

Model	ExpDecay1
Equation	y = y0 + A1*exp(-(x-x0)/t1)
Plot	current
y0	0,00238 ± 0
x0	4,14025 ± 0
A1	-5,3841E-4 ± 1,1468E-5
t1	0,1857 ± 0,00588
Reduced Chi-Sqr	1,58938E-9
R-Square(COD)	0,92366
Adj. R-Square	0,92311

Model	ExpDecay1
Equation	y = y0 + A1*exp(-(x-x0)/t1)
Plot	current
y0	-0,00186 ± 0
x0	4,67898 ± 0
A1	-4,11021E-4 ± 1,92253E-5
t1	0,05212 ± 0,00416
Reduced Chi-Sqr	2,51065E-9
R-Square(COD)	0,81905
Adj. R-Square	0,81782

Figure S6 Fitting data of exponential function fitted to learning (right panel) and forgetting (left panel).

5. Electric impulses sequences

Here, in we present voltage sequences for most crucial experiments in current publication. Voltage levels have been established empirically, based on preliminary tests for each type of sample (Figure S7a, b, c).

a. **Voltage sequence for I-V hysteresis -** before main neuromorphic measurements for each sample, each sample was tested with I-V scans – several, typically 20 voltage scans, within -3.5 V to 3.5 V range, with moderate scan speed – 200 mV/s.

b. **Sequence for STDP measurements -** typically, each sample was measured 3 times for each Δt value.

c. **Sequence for SRDP measurements**

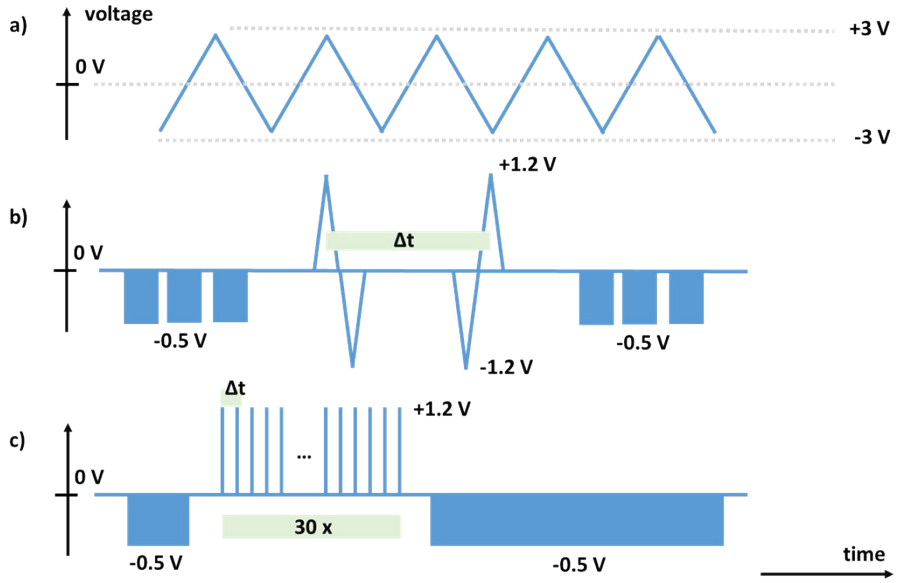

Figure S7 Voltage sequences used in I-V hysteresis curve experiment (a), STDP experiments – in case of $\Delta t < 0$, the two spikes exchange places (b), SRDP experiments (c).

6. STDP – DC bias results for negative Δt (LTD regime)

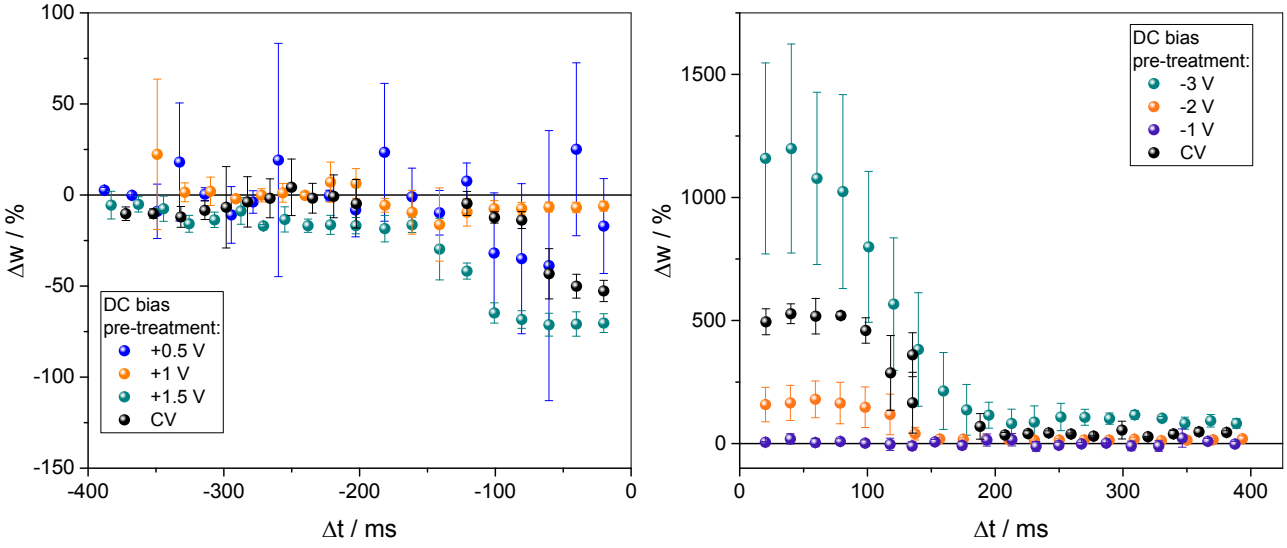

Figure S8 STDP curve comparison between conventional experiments (CV scan performed before the poling spikes sequence) and experiments with the priming activity (DC bias pre-treatment before the sequence). The figure shows results of two plasticity regimes – left part is for depression regime (LTD) and the right part is for potentiation regime (LTP).

7. STDP – non-volatile learning

In Figure S9 we present the direct transition into LTP regime after the STDP measurement.

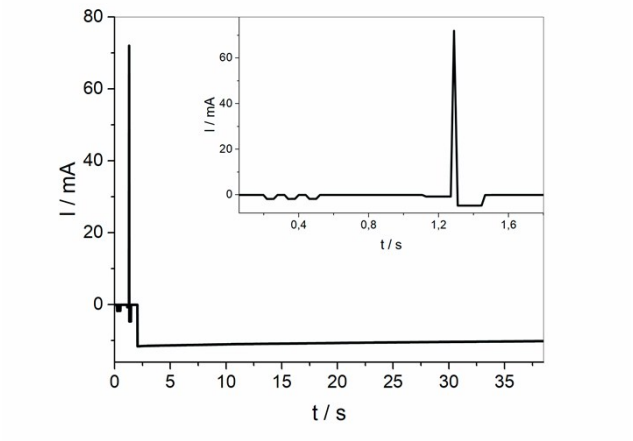

Figure S9 STDP measured as current response for 36 s after applying pair of spikes with Δt = 20 ms. No significant change in current suggests that observed effect belongs to LTP regime. Before poling the sample current was read three times at -0.5 V (depicted in inset).

8. SRDP measured for materials made with different MAI:BiI_3 ratio.

The SRDP of the two least defected samples, i.e. MABiI 1:1 and 3:2, can be described with single exponential function. The long time constant τ_l (the constant is called "long" for the sake of the further discussion) for MABiI 3:2 is 560±397 ms and 533±210 ms for MABiI 1:1. However this fit is not ideal due to significant scatter of the data points, the tendency is quite explicit. In the range of the estimated uncertainty both time constants can be considered as equal (Figure S10).

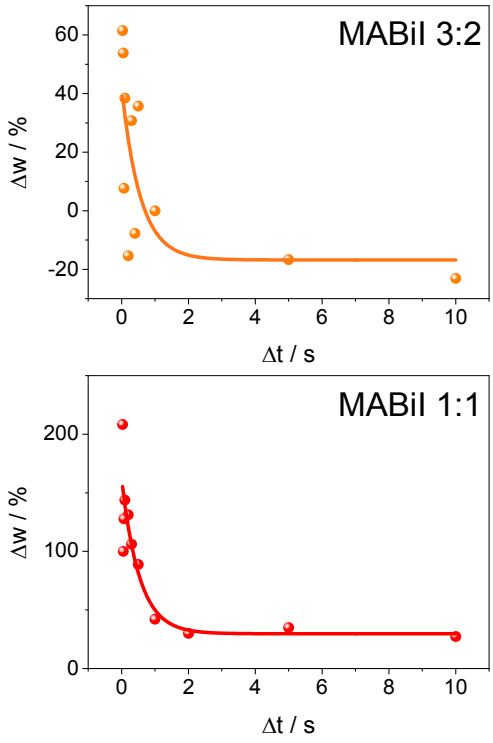

Model	ExpDecay1
Equation	y = y0 + A1*exp(-(x-x0)
Plot	3:2
y0	-16.79082 ± 0
x0	-0.10459 ± 0
A1	71.09364 ± 25.10971
t1	0.55986 ± 0.39763
Reduced Chi-Sq	513.07134
R-Square(COD)	0.49101
Adj. R-Square	0.43446

Model	ExpDecay1
Equation	y = y0 + A1*exp(-(x-x0)
Plot	1:1
y0	29.70713 ± 0
x0	-0.0737 ± 0
A1	152.63723 ± 25.91378
t1	0.53264 ± 0.2096
Reduced Chi-Sq	666.46867
R-Square(COD)	0.81827
Adj. R-Square	0.79808

Figure S10 Single-exponent functions fitted to MABil 1:1 and 3:2 samples in SRDP measurement.

However, this simple exponential function doesn't describe well the data collected for MABil 1:3 and 3:1. The closer look at the data collected for this samples reveals that the data can be better described with a more sophisticated equation consisting of the following form:

$$I = \begin{cases} I_0 + A_d + A_g\left(e^{-\frac{t_c}{\tau_s}} - e^{-\frac{t}{\tau_l}}\right) & t < t_c \\ I_0 + A_d e^{-(t-t_c)/\tau_l} & t > t_c \end{cases} \quad (3)$$

where y_o is the reading current offset, A_d and A_g are amplitudes for growth and decay region of the function, t_c is the time interval value with the highest current amplitude, τ_s and τ_l are the short and long time constants, respectively.

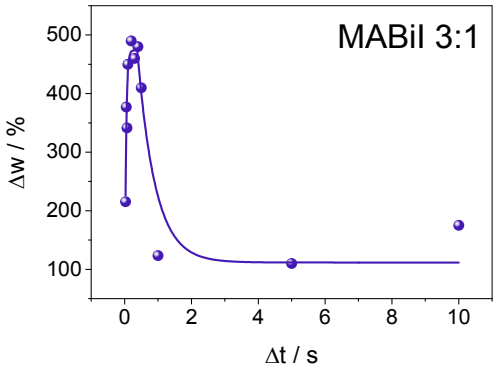

Model	ExpGrowDec
Equation	y = x<xc ? y0+Ad+Ag*(exp(-xc/tg)-exp(-x/tg)) : y0+Ad*exp(-(x-xc)/td);
Plot	3:1
y0	111.67264 ± 44.81469
xc	0.37992 ± 0.11006
Ag	566.49488 ± 356.91897
tg	0.03619 ± 0.02439
Ad	362.25289 ± 64.00157
td	0.53264 ± 0.30254
Reduced Chi-Sqr	4021.37584
R-Square(COD)	0.90705
Adj. R-Square	0.81411

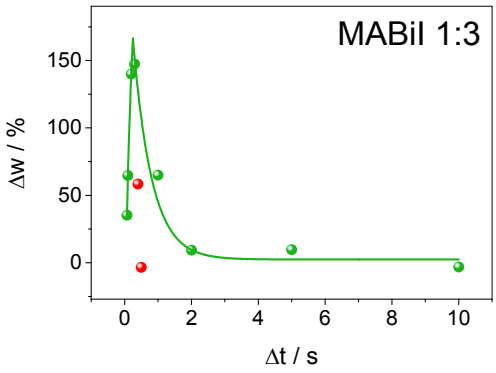

Model	ExpGrowDec
Equation	y = x<xc ? y0+Ad+Ag*(exp(-xc/tg)-exp(-x/tg)) : y0+Ad*exp(-(x-xc)/td);
Plot	1:3
y0	2.40152 ± 0
xc	0.24871 ± 0.0506
Ag	333.4306 ± 435.86766
tg	0.23727 ± 0.69672
Ad	164.21751 ± 16.73121
td	0.55986 ± 0.12884
Reduced Chi-Sqr	164.58121
R-Square(COD)	0.97921
Adj. R-Square	0.95149

Figure S11 Two-exponential function fitting for MABil 3:1 and 1:3 samples in SRDP measurement. The points marked in red were excluded from the fitting procedure and *y_0 parameter (y-axis offset) was fixed in the fit for MABil 1:3*.

This suggests that for more defected samples another process with different time constant occurs with a significantly shorter time constant. The estimated constants are τ_l = 533±303 ms and τ_s = 36±24 ms for MABil 3:1 and τ_l = 560±129 ms and τ_s = 237±697 ms for MABil 1:3. However the fits are far from being perfect and should be treated rather as qualitative than a quantitative experiment, the presence of the short time constant is obvious in the mentioned samples. To improve the output of the measurement, we suggest that sputtered electrodes and current compliance should be introduced to reduce the data points scatter.

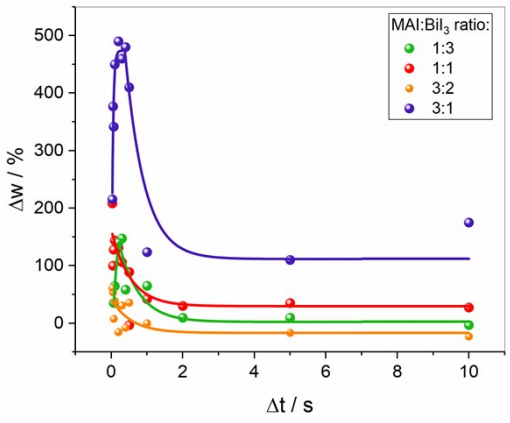

Figure S12 Collective graph of SRDP measurement output for different MAI:BiI_3 with fitted functions.

The presence of two significantly different time constants indicated the possibility of material evolution, i.e. relaxation processes that change the occupancy of the trap states and hence the conductivity and synaptic weights. The presence of two types of electron traps with different dynamics (trapping time) might also be significant in memory consolidation process. Once again, we conclude that more defected materials presented higher and more stable synaptic weight changes, proving indirectly the significant role of lattice defects in the charge trapping processes and hence the observed memristive effects. It does not exclude, however the role of ion migration, as it has already been postulated for stoichiometric samples of MABiI.

Bibliography:

1 M. Hansen, M. Ziegler, L. Kolberg, R. Soni, S. Dirkmann, T. Mussenbrock and H. Kohlstedt, *Sci. Rep.*, 2015, **5**, 13753.

2 M. Pazoki, M. B. Johansson, H. Zhu, P. Broqvist, T. Edvinsson, G. Boschloo and E. M. J. Johansson, *J. Phys. Chem. C*, 2016, **120**, 29039–29046.